

# Developing a time-domain finite-element method for modeling of electromagnetic cylindrical cloaks

Jichun Li <sup>a,b,\*</sup>, Yunqing Huang <sup>a,2</sup>, Wei Yang <sup>a,3</sup>

<sup>a</sup> Hunan Key Laboratory for Computation and Simulation in Science and Engineering, Xiangtan University, Xiangtan 411105, China

<sup>b</sup> Department of Mathematical Sciences, University of Nevada Las Vegas, Las Vegas, NV 89154-4020, USA

## ARTICLE INFO

### Article history:

Received 9 September 2011

Received in revised form 21 November 2011

Accepted 25 December 2011

Available online 4 January 2012

### Keywords:

Maxwell's equations

Invisibility cloak

Finite element method

## ABSTRACT

In this paper we propose a time-domain finite element method for modeling of electromagnetic cloaks. The permittivity and permeability of the cloak model are described by the Drude dispersion model. The model to be solved is quite challenging in that we have to solve a coupled problem with different partial differential equations given in different regions. Our method is based on a mixed finite element method using edge elements with different types of meshes in different regions. Numerical results demonstrate that our algorithm is quite effective for simulating cloaks in time-domain. To our knowledge, this is the first cloak simulation carried out by the time-domain finite element method.

© 2012 Elsevier Inc. All rights reserved.

## 1. Introduction

The possibility of cloaking an object from detection by electromagnetic waves has recently become a very hot research topic. In 2006, Pendry et al. [25] and Leonhardt [14] independently showed that it is possible to create invisible cloaks for ray optics [14] and electromagnetic waves [25] by guiding light around a region as if nothing is there. In late 2006, a 2-D reduced cloak was successfully fabricated and demonstrated to work in the microwave frequency region [26]. This is the first practical realization of such a cloak, and the result matches with the computer simulation [6] performed using COMSOL multiphysics finite element analysis software. These pioneering work inspired researchers in different disciplines around the world to pursue the human being's invisibility dream.

Since 2006, many papers have been published on the study of using metamaterials [3,8,18] to construct invisibility cloaks of different shapes (e.g. [1,5,21,22,28]). Also cloaks operating from microwave frequencies to optical frequencies have been achieved, more details and references on cloaking can be found in recent reviews [4,9]. Some mathematical analysis has been carried out for cloaking in frequency domain [19,13].

Numerical simulation plays a very important role in modeling different cloaks and validating theoretical predictions. The time-domain finite difference (FDTD) method is a very popular technique used in this area, readers can find more details about the FDTD method and its applications in cloak simulation in a recent book [10]. Due to the major disadvantage of FDTD method in dealing with complex geometry [30], the finite element method (FEM) based commercial package COMSOL has

\* Corresponding author at: Department of Mathematical Sciences, University of Nevada Las Vegas, Las Vegas, NV 89154-4020, USA. Tel.: +1 (702) 895 0355.

E-mail addresses: [jichun@unlv.nevada.edu](mailto:jichun@unlv.nevada.edu) (J. Li), [huangyq@xtu.edu.cn](mailto:huangyq@xtu.edu.cn) (Y. Huang), [yangweixtu@126.com](mailto:yangweixtu@126.com) (W. Yang).

<sup>1</sup> Supported by National Science Foundation Grant DMS-0810896.

<sup>2</sup> This work was supported by National Science Foundation Grant DMS-0810896, and in part by the NSFC Key Project 11031006 and Hunan Provincial NSF project 10JJ7001.

<sup>3</sup> Supported by Hunan Education Department Key Project 10A117 and Hunan Provincial Innovation Foundation for Postgraduate (CX2011B243).

been extensively used in frequency-domain cloak simulation by engineers and physicists [6,4]. However, COMSOL cannot be used for time-domain cloak simulation due to its limitation on algorithmic development for time-domain cloak modeling. On the other hand, the recently designed broadband cloaks [20] make the time-domain simulation more appealing and necessary. But little attention has been paid to the time-domain modeling of cloaks. To our best knowledge, the first time-domain simulation of 2-D cloaking structures was carried out by Zhao et al. [31] in 2008 using FDTD method. Later, they generalized the same idea to 3-D cloak simulation in 2009 [32]. It seems that there is no existing work on time-domain finite element (FETD) method developed for cloak simulation yet.

In this paper, we propose a FETD method to simulate a 2-D cylindrical cloak. This problem is quite challenging, since we have to solve a coupled problem with different partial differential equations in different regions, and the material parameters are highly anisotropic and nonhomogeneous. The rest of the paper is organized as follows. We first describe the 2-D cylindrical cloak modeling equations in Section 2. In Section 3, we develop a FETD method for solving the model problem. Then in Section 4, we present a detailed stability analysis of our scheme. Numerical results showing the cloaking phenomena obtained by our method are illustrated in Section 5. We conclude the paper in Section 6.

## 2. The modeling equations

The cloak modeling is based on the Faraday’s law and Ampere’s law written as follows:

$$\frac{\partial \mathbf{B}}{\partial t} = -\nabla \times \mathbf{E}, \tag{1}$$

$$\frac{\partial \mathbf{D}}{\partial t} = \nabla \times \mathbf{H} \tag{2}$$

and the constitutive relations

$$\mathbf{D} = \varepsilon \mathbf{E}, \tag{3}$$

$$\mathbf{B} = \mu \mathbf{H}, \tag{4}$$

where  $\mathbf{E}$  and  $\mathbf{H}$  are the electric and magnetic fields respectively,  $\mathbf{D}$  and  $\mathbf{B}$  are the electric displacement and magnetic induction respectively,  $\varepsilon$  and  $\mu$  are cloak permittivity and permeability, respectively. For the cylindrical cloak, the ideal material parameters in the polar coordinate system are given by [25]:

$$\varepsilon_r = \mu_r = \frac{r - R_1}{r}, \quad \varepsilon_\phi = \mu_\phi = \frac{r}{r - R_1}, \quad \varepsilon_z = \mu_z = \left(\frac{R_2}{R_2 - R_1}\right)^2 \frac{r - R_1}{r}, \tag{5}$$

where  $R_1$  and  $R_2$  are the inner and outer radius of the cloak. In this case,  $\mathbf{E}$  becomes a 2-D vector, and  $\mathbf{H}$  is a scalar, i.e., we can write  $\mathbf{E} = (E_x, E_y)'$  and  $H = H_z$ , where the subindex  $x, y$  or  $z$  denotes the component in each direction.

Transforming the polar coordinate system to the Cartesian coordinate system, we can obtain [31]:

$$\varepsilon_0 \varepsilon_r \varepsilon_\phi \mathbf{E} = \begin{bmatrix} \varepsilon_r \sin^2 \phi + \varepsilon_\phi \cos^2 \phi & (\varepsilon_\phi - \varepsilon_r) \sin \phi \cos \phi \\ (\varepsilon_\phi - \varepsilon_r) \sin \phi \cos \phi & \varepsilon_r \cos^2 \phi + \varepsilon_\phi \sin^2 \phi \end{bmatrix} \mathbf{D}. \tag{6}$$

Because the material parameters given in (5) can not be used directly to simulate the time-domain cloak, we have to map the parameters using the dispersive medium models. Here we consider the Drude model for the permittivity:

$$\varepsilon_r(\omega) = 1 - \frac{\omega_p^2}{\omega^2 - j\omega\gamma}, \tag{7}$$

where  $\gamma \geq 0$  and  $\omega_p > 0$  are the collision and plasma frequencies, respectively. Substituting (7) into (6) and using the following rules

$$j\omega \rightarrow \frac{\partial}{\partial t}, \quad \omega^2 \rightarrow -\frac{\partial^2}{\partial t^2}, \tag{8}$$

we have (detailed derivation see [31]):

$$\varepsilon_0 \varepsilon_\phi \left( \frac{\partial^2}{\partial t^2} + \gamma \frac{\partial}{\partial t} + \omega_p^2 \right) \mathbf{E} = \left( \frac{\partial^2}{\partial t^2} + \gamma \frac{\partial}{\partial t} + \omega_p^2 \right) M_A \mathbf{D} + \varepsilon_\phi \left( \frac{\partial^2}{\partial t^2} + \gamma \frac{\partial}{\partial t} \right) M_B \mathbf{D}, \tag{9}$$

where we denote  $\mathbf{D} = (D_x, D_y)'$  and

$$M_A = \begin{bmatrix} \sin^2 \phi & -\sin \phi \cos \phi \\ -\sin \phi \cos \phi & \cos^2 \phi \end{bmatrix}, \quad M_B = \begin{bmatrix} \cos^2 \phi & \sin \phi \cos \phi \\ \sin \phi \cos \phi & \sin^2 \phi \end{bmatrix}.$$

Similarly, we map the permeability using the Drude model [31]:

$$\mu_z(\omega) = A \left( 1 - \frac{\omega_{pm}^2}{\omega^2 - j\omega\gamma_m} \right), \tag{10}$$

where  $A = \frac{k_2}{k_2 - k_1}$ , and  $\omega_{pm} > 0$  and  $\gamma_m \geq 0$  are the magnetic plasma and collision frequencies, respectively. Substituting (10) into (4), we obtain

$$B_z = \mu_0 \mu_z H_z = \mu_0 A \left( 1 - \frac{\omega_{pm}^2}{\omega^2 - j\omega\gamma_m} \right) H_z.$$

Then using rules (8), we have

$$\left( \frac{\partial^2}{\partial t^2} + \gamma_m \frac{\partial}{\partial t} \right) B_z = \mu_0 A \left( \frac{\partial^2}{\partial t^2} + \gamma_m \frac{\partial}{\partial t} + \omega_{pm}^2 \right) H_z. \tag{11}$$

To carry out the cloak simulation, we have to reduce the infinite domain problem to a bounded domain by using Berenger’s perfectly matched layer (PML) [2] to absorb waves leaving the computational domain without introducing reflections. The two dimensional Berenger PML governing equations can be written as:

$$\epsilon_0 \frac{\partial E_x}{\partial t} + \sigma_y E_x = \frac{\partial (H_{zx} + H_{zy})}{\partial y}, \tag{12}$$

$$\epsilon_0 \frac{\partial E_y}{\partial t} + \sigma_x E_y = -\frac{\partial (H_{zx} + H_{zy})}{\partial x}, \tag{13}$$

$$\mu_0 \frac{\partial H_{zx}}{\partial t} + \sigma_{mx} H_{zx} = -\frac{\partial E_y}{\partial x}, \tag{14}$$

$$\mu_0 \frac{\partial H_{zy}}{\partial t} + \sigma_{my} H_{zy} = \frac{\partial E_x}{\partial y}, \tag{15}$$

where the parameters  $\sigma_i, \sigma_{mi}, i = x, y$ , are the homogeneous electric and magnetic conductivities in the  $x$  and  $y$  directions, respectively.

For easy implementation of our algorithm given below, we rewrite (12) and (13) in the vector form:

$$\epsilon_0 \frac{\partial \mathbf{E}}{\partial t} + \begin{pmatrix} \sigma_y & 0 \\ 0 & \sigma_x \end{pmatrix} \mathbf{E} = \nabla \times H, \tag{16}$$

where we used the 2-D vector curl operator

$$\nabla \times H = \begin{pmatrix} \frac{\partial H}{\partial y} \\ -\frac{\partial H}{\partial x} \end{pmatrix}, \quad \text{for } H = H_{zx} + H_{zy}.$$

### 3. A fully discrete explicit finite element scheme

To design our mixed finite element method, we partition  $\Omega$  by a family of regular meshes  $T^h$  with maximum mesh size  $h$ . To accommodate our problem easily, we use a mesh with mixed types of elements: triangles in the cloak and free space region; rectangles in the PML region, cf. Fig. 1(b) below. For simplicity, currently we implement our algorithm using the lowest-order Raviart–Thomas–Nédélec’s mixed spaces  $\mathbf{U}_h$  and  $\mathbf{V}_h$  given as follows [23,24]: for any rectangular element  $K \in T^h$ , we choose

$$\begin{aligned} \mathbf{U}_h &= \left\{ \psi_h \in L^2(\Omega) : \psi_h|_K \in Q_{0,0}, \forall K \in T^h \right\}, \\ \mathbf{V}_h &= \left\{ \phi_h \in H(\text{curl}; \Omega) : \phi_h|_K \in Q_{0,1} \times Q_{1,0}, \forall K \in T^h \right\}, \end{aligned}$$

where  $Q_{ij}$  denotes the space of polynomials whose degrees are less than or equal to  $i$  and  $j$  in variables  $x$  and  $y$ , respectively. Here we denote the space  $H(\text{curl}; \Omega) = \{ \mathbf{v} \in (L^2(\Omega))^2; \nabla \times \mathbf{v} \in (L^2(\Omega))^2 \}$ . While on a triangular element, we choose

$$\begin{aligned} \mathbf{U}_h &= \left\{ \psi_h \in L^2(\Omega) : \psi_h|_K \text{ is a piecewise constant}, \forall K \in T^h \right\}, \\ \mathbf{V}_h &= \left\{ \phi_h \in H(\text{curl}; \Omega) : \phi_h|_K = \text{span}\{ \lambda_i \nabla \lambda_j - \lambda_j \nabla \lambda_i \}, i, j = 1, 2, 3, \forall K \in T^h \right\}, \end{aligned}$$

where  $\lambda_i$  denotes the standard linear basis function at vertex  $i$  of element  $K$ .

To impose the perfect conducting boundary condition  $\mathbf{n} \times \mathbf{E} = \mathbf{0}$ , we introduce the space

$$\mathbf{V}_h^0 = \{ \phi_h \in \mathbf{V}_h, \mathbf{n} \times \phi_h = \mathbf{0} \text{ on } \partial\Omega \}.$$

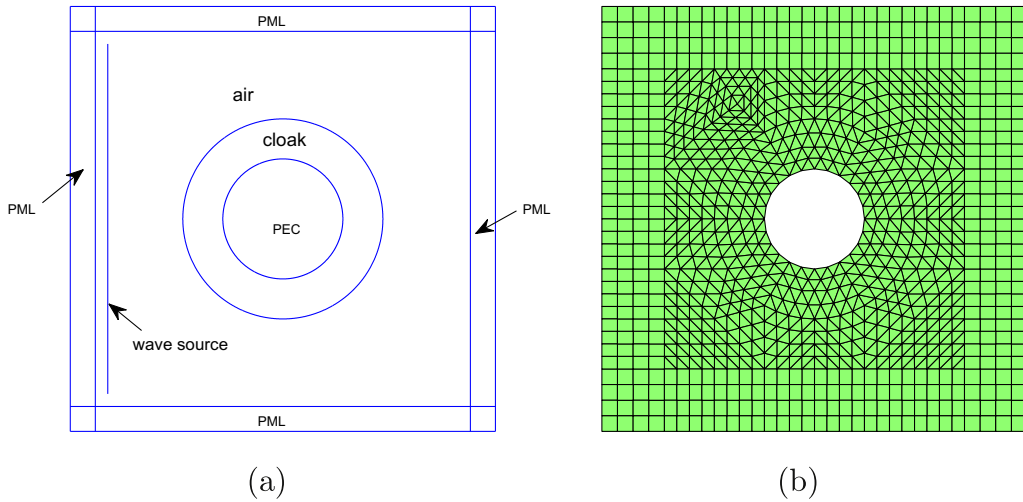


Fig. 1. (a) The cloak modeling setup; and (b) a coarse mesh.

To define a fully-discrete scheme, we divide the time interval  $I = [0, T]$  into  $N$  uniform subintervals  $I_i = [t_{i-1}, t_i]$  by points  $t_i = i\tau$ ,  $i = 0, 1, \dots, N$ , where  $\tau = T/N$ . Furthermore, we denote  $\mathbf{u}^n = \mathbf{u}(\cdot, t_n)$  and  $\mathbf{u}^{n+\frac{1}{2}} = \mathbf{u}(\cdot, (n + \frac{1}{2})\tau)$ , and introduce some operators:

$$\begin{aligned} \delta_\tau \mathbf{u}^n &= \frac{\mathbf{u}^n - \mathbf{u}^{n-1}}{\tau}, & \delta_\tau^2 \mathbf{u}^n &= \frac{\mathbf{u}^n - 2\mathbf{u}^{n-1} + \mathbf{u}^{n-2}}{\tau^2}, \\ \delta_{2\tau} \mathbf{u}^n &= \frac{\mathbf{u}^n - \mathbf{u}^{n-2}}{2\tau}, & \bar{\mathbf{u}}^{n-1} &= \frac{\mathbf{u}^n + 2\mathbf{u}^{n-1} + \mathbf{u}^{n-2}}{4}, & \hat{\mathbf{u}}^n &= \frac{\mathbf{u}^n + \mathbf{u}^{n-1}}{2}. \end{aligned}$$

With the above preparation, we now construct a leap-frog type scheme for solving the modeling equations in the cloak region: for  $n = 1, 2, \dots$ , find  $\mathbf{D}_h^{n+\frac{1}{2}}, \mathbf{E}_h^{n+\frac{1}{2}} \in \mathbf{V}_h, \mathbf{B}_h^{n+1}, H_h^{n+1} \in U_h$  such that

$$(\delta_\tau \mathbf{D}_h^{n+\frac{1}{2}}, \phi_h) - (H_h^n, \nabla \times \phi_h) = 0, \tag{17}$$

$$\begin{aligned} &(\varepsilon_0 \varepsilon_\phi \delta_\tau^2 \mathbf{E}_h^{n+\frac{1}{2}}, \tilde{\phi}_h) + (\gamma \varepsilon_0 \varepsilon_\phi \delta_{2\tau} \mathbf{E}_h^{n+\frac{1}{2}}, \tilde{\phi}_h) + (\omega_p^2 \varepsilon_0 \varepsilon_\phi \bar{\mathbf{E}}_h^{n-\frac{1}{2}}, \tilde{\phi}_h) \\ &= ((M_A + \varepsilon_\phi M_B) \delta_\tau^2 \mathbf{D}_h^{n+\frac{1}{2}}, \tilde{\phi}_h) + (\omega_p^2 M_A \bar{\mathbf{D}}_h^{n-\frac{1}{2}}, \tilde{\phi}_h) + (\gamma (M_A + \varepsilon_\phi M_B) \delta_{2\tau} \mathbf{D}_h^{n+\frac{1}{2}}, \tilde{\phi}_h), \end{aligned} \tag{18}$$

$$(\delta_\tau \mathbf{B}_h^{n+1}, \psi_h) + (\nabla \times \mathbf{E}_h^{n+\frac{1}{2}}, \psi_h) = 0, \tag{19}$$

$$(\mu_0 A \delta_\tau^2 H_h^{n+1}, \tilde{\psi}_h) + (\mu_0 A \gamma_m \delta_{2\tau} H_h^{n+1}, \tilde{\psi}_h) + (\mu_0 A \omega_{pm}^2 \bar{H}_h^n, \tilde{\psi}_h) = (\delta_\tau^2 \mathbf{B}_h^{n+1}, \tilde{\psi}_h) + (\gamma_m \delta_{2\tau} \mathbf{B}_h^{n+1}, \tilde{\psi}_h) \tag{20}$$

hold true for any  $\phi_h, \tilde{\phi}_h \in \mathbf{V}_h^0, \psi_h, \tilde{\psi}_h \in U_h$ .

In order to couple (20) well with the PML Eqs. (14) and (15), we split (20) into

$$(\mu_0 A \delta_\tau^2 H_{zx,h}^{n+1}, \tilde{\psi}_h) + (\mu_0 A \gamma_m \delta_{2\tau} H_{zx,h}^{n+1}, \tilde{\psi}_h) + (\mu_0 A \omega_{pm}^2 \bar{H}_{zx,h}^n, \tilde{\psi}_h) = \frac{1}{2} (\delta_\tau^2 \mathbf{B}_h^{n+1}, \tilde{\psi}_h) + \frac{1}{2} (\gamma_m \delta_{2\tau} \mathbf{B}_h^{n+1}, \tilde{\psi}_h), \tag{21}$$

$$(\mu_0 A \delta_\tau^2 H_{zy,h}^{n+1}, \tilde{\psi}_h) + (\mu_0 A \gamma_m \delta_{2\tau} H_{zy,h}^{n+1}, \tilde{\psi}_h) + (\mu_0 A \omega_{pm}^2 \bar{H}_{zy,h}^n, \tilde{\psi}_h) = \frac{1}{2} (\delta_\tau^2 \mathbf{B}_h^{n+1}, \tilde{\psi}_h) + \frac{1}{2} (\gamma_m \delta_{2\tau} \mathbf{B}_h^{n+1}, \tilde{\psi}_h). \tag{22}$$

Similarly, we can construct a leap-frog type scheme for solving the Eqs. (16), (14) and (15) in the PML region: find  $\mathbf{E}_h^{n+\frac{1}{2}} \in \mathbf{V}_h, H_{zx,h}^{n+1}, H_{zy,h}^{n+1} \in U_h$  such that

$$\varepsilon_0 (\delta_\tau \mathbf{E}_h^{n+\frac{1}{2}}, \tilde{\phi}_h) + \left( \begin{pmatrix} \sigma_y & 0 \\ 0 & \sigma_x \end{pmatrix} \hat{\mathbf{E}}_h^{n+\frac{1}{2}}, \tilde{\phi}_h \right) = (H_{zx,h}^n + H_{zy,h}^n, \nabla \times \tilde{\phi}_h), \tag{23}$$

$$\mu_0 (\delta_\tau H_{zx,h}^{n+1}, \psi_{1,h}) + (\sigma_{mx} \hat{H}_{zx,h}^{n+1}, \psi_{1,h}) = - \left( \frac{\partial}{\partial X} \mathbf{E}_{y,h}^{n+\frac{1}{2}}, \psi_{1,h} \right), \tag{24}$$

$$\mu_0 \left( \delta_\tau H_{zy,h}^{n+1}, \psi_{2,h} \right) + \left( \sigma_{my} \widehat{H}_{zy,h}^{n+1}, \psi_{2,h} \right) = \left( \frac{\partial}{\partial \mathbf{y}} E_{x,h}^{n+\frac{1}{2}}, \psi_{2,h} \right) \tag{25}$$

hold true for any  $\tilde{\phi}_h \in \mathbf{V}_h^0, \psi_{1,h}, \psi_{2,h} \in U_h$ .

In summary, our mixed finite element time-domain algorithm for modeling the invisible cloak can be performed in the following steps: first, construct a proper mesh  $\mathcal{T}_h$  of  $\Omega$ , choose a proper time step size  $\tau$  and proper initial conditions; then at each time step  $n$ , perform the **FETD Algorithm**:

1. Solve (17) for  $\mathbf{D}_h^{n+\frac{1}{2}}$  on  $\mathcal{T}_h$ .
2. Solve (18) and (23) for  $\mathbf{E}_h^{n+\frac{1}{2}}$  on  $\mathcal{T}_h$ .
3. Solve (19) for  $\mathbf{B}_h^{n+1}$  on  $\mathcal{T}_h$ .
4. Solve (21) and (24) for  $H_{zx,h}^{n+1}$  on  $\mathcal{T}_h$ .
5. Solve (22) and (25) for  $H_{zy,h}^{n+1}$  on  $\mathcal{T}_h$ .
6. Calculate  $H_h^{n+1} = H_{zx,h}^{n+1} + H_{zy,h}^{n+1}$ , then go back to step 1 and repeat the above process. Note that in the free space region,  $\mathbf{E}_h^{n+\frac{1}{2}}$  and  $H^{n+1}$  are updated using (23)–(25) with  $\sigma_x = \sigma_y = \sigma_{mx} = \sigma_{my} = 0$ .

#### 4. Stability analysis

In this section, we present the stability analysis for our proposed scheme. Let  $c_v = 1/\sqrt{\epsilon_0 \mu_0}$  be the wave propagation speed in vacuum,  $c_{inv} > 0$  is a constant from the inverse estimate

$$\|\nabla \times \psi_h\|_{0,\Omega} \leq c_{inv} h^{-1} \|\psi_h\|_{0,\Omega}, \quad \forall \psi_h \in \mathbf{V}_h, \tag{26}$$

where  $\|\cdot\|_{0,\Omega}$  denotes the  $L^2$  norm over domain  $\Omega$ .

We start with the easy stability analysis in the PML and free space region  $\Omega_r$ :

**Theorem 4.1.** Assume that the time step

$$\tau \leq \frac{h}{c_v c_{inv}}, \tag{27}$$

then for any  $n \geq 2$  and the solution  $(\mathbf{E}_h^{n-\frac{1}{2}}, H_h^n = (H_{zx,h}^n, H_{zy,h}^n))$  of (23)–(25), we have

$$\epsilon_0 \left\| \mathbf{E}_h^{n-\frac{1}{2}} \right\|_{0,\Omega_r}^2 + \mu_0 \|H_h^n\|_{0,\Omega_r}^2 \leq 3 \left( \epsilon_0 \left\| \mathbf{E}_h^{\frac{1}{2}} \right\|_{0,\Omega_r}^2 + \mu_0 \|H_h^1\|_{0,\Omega_r}^2 \right),$$

where we denote  $\|H_h^n\|_{0,\Omega_r}^2 = \|H_{zx,h}^n\|_{0,\Omega_r}^2 + \|H_{zy,h}^n\|_{0,\Omega_r}^2$ .

**Proof.** Choosing  $\tilde{\phi}_h = 2\tau \widehat{\mathbf{E}}_h^{n+\frac{1}{2}}, \psi_{1,h} = 2\tau \widehat{H}_{zx,h}^{n+1}$  and  $\psi_{2,h} = 2\tau \widehat{H}_{zy,h}^{n+1}$  in (23)–(25), respectively, and using the 2-D curl notation, we obtain

$$\begin{aligned} & \epsilon_0 \left( \left\| \mathbf{E}_h^{n+\frac{1}{2}} \right\|_{0,\Omega_r}^2 - \left\| \mathbf{E}_h^{n-\frac{1}{2}} \right\|_{0,\Omega_r}^2 \right) + \mu_0 \left( \left\| H_h^{n+1} \right\|_{0,\Omega_r}^2 - \left\| H_h^n \right\|_{0,\Omega_r}^2 \right) \leq 2\tau \left( \left( H_h^n, \nabla \times \widehat{\mathbf{E}}_h^{n+\frac{1}{2}} \right) - \left( \nabla \times \mathbf{E}_h^{n+\frac{1}{2}}, \widehat{H}_h^{n+1} \right) \right) \\ & = \tau \left( \left( H_h^n, \nabla \times \mathbf{E}_h^{n-\frac{1}{2}} \right) - \left( H_h^{n+1}, \nabla \times \mathbf{E}_h^{n+\frac{1}{2}} \right) \right), \end{aligned} \tag{28}$$

where in the last step we used the identity

$$\left( H_h^n, \nabla \times \left( \mathbf{E}_h^{n+\frac{1}{2}} + \mathbf{E}_h^{n-\frac{1}{2}} \right) \right) - \left( \nabla \times \mathbf{E}_h^{n+\frac{1}{2}}, H_h^{n+1} + H_h^n \right) = \left( H_h^n, \nabla \times \mathbf{E}_h^{n-\frac{1}{2}} \right) - \left( H_h^{n+1}, \nabla \times \mathbf{E}_h^{n+\frac{1}{2}} \right).$$

Summing up (28) from  $n = 1$  to  $N - 1$ , we obtain

$$\epsilon_0 \left( \left\| \mathbf{E}_h^{N-\frac{1}{2}} \right\|_{0,\Omega_r}^2 - \left\| \mathbf{E}_h^{\frac{1}{2}} \right\|_{0,\Omega_r}^2 \right) + \mu_0 \left( \left\| H_h^N \right\|_{0,\Omega_r}^2 - \left\| H_h^1 \right\|_{0,\Omega_r}^2 \right) \leq \tau \left( \left( H_h^1, \nabla \times \mathbf{E}_h^{\frac{1}{2}} \right) - \left( H_h^N, \nabla \times \mathbf{E}_h^{N-\frac{1}{2}} \right) \right). \tag{29}$$

Using the definition  $c_v = 1/\sqrt{\epsilon_0 \mu_0}$ , the inverse estimate (26), the Cauchy–Schwarz inequality, and the time constraint (27), we have

$$\begin{aligned} \tau \left( H_h^N, \nabla \times \mathbf{E}_h^{N-\frac{1}{2}} \right) &= \left( \sqrt{\mu_0} H_h^N, \tau c_v \sqrt{\epsilon_0} \nabla \times \mathbf{E}_h^{N-\frac{1}{2}} \right) \leq \frac{1}{2} \left( \mu_0 \|H_h^N\|_{0,\Omega_r}^2 + (\tau c_v)^2 \epsilon_0 \left\| \nabla \times \mathbf{E}_h^{N-\frac{1}{2}} \right\|_{0,\Omega_r}^2 \right) \\ &\leq \frac{1}{2} \left( \mu_0 \|H_h^N\|_{0,\Omega_r}^2 + (\tau c_v c_{inv} h^{-1})^2 \epsilon_0 \left\| \mathbf{E}_h^{N-\frac{1}{2}} \right\|_{0,\Omega_r}^2 \right) \leq \frac{1}{2} \mu_0 \|H_h^N\|_{0,\Omega_r}^2 + \frac{1}{2} \epsilon_0 \left\| \mathbf{E}_h^{N-\frac{1}{2}} \right\|_{0,\Omega_r}^2. \end{aligned} \tag{30}$$

By the same technique, we obtain

$$\tau \left( H_h^1, \nabla \times E_h^1 \right) \leq \frac{1}{2} \mu_0 \| H_h^1 \|_{0,\Omega_r}^2 + \frac{1}{2} \epsilon_0 \| E_h^1 \|_{0,\Omega_r}^2. \tag{31}$$

Substituting the estimates (30) and (31) into (29) completes the proof.  $\square$

**Remark 4.1.** To see how large  $c_{inv}$  in (26) can be, let us consider an arbitrary rectangular element  $K = [x_c - h_x, x_c + h_x] \times [y_c - h_y, y_c + h_y]$ , on which the lowest edge element basis functions are:

$$\psi_1^h = \begin{pmatrix} \frac{(y_c+h_y)-y}{4h_x h_y} \\ 0 \end{pmatrix}, \quad \psi_2^h = \begin{pmatrix} 0 \\ \frac{x-(x_c-h_x)}{4h_x h_y} \end{pmatrix}, \quad \psi_3^h = \begin{pmatrix} \frac{(y_c-h_y)-y}{4h_x h_y} \\ 0 \end{pmatrix}, \quad \psi_4^h = \begin{pmatrix} 0 \\ \frac{x-(x_c+h_x)}{4h_x h_y} \end{pmatrix}.$$

Here  $\psi_j^h$ ,  $j = 1, 2, 3, 4$ , start from the bottom edge and orient counterclockwisely.

For simplicity, we assume that the mesh  $T^h$  of  $\Omega$  is formed by  $N$  rectangles  $K$ . In this case, it is easy to check that the 2D curl of  $\psi_j^h$  satisfies

$$\int_{\Omega} |\nabla \times \psi_j^h|^2 dx dy = \sum_{K \in T^h} \int_K \left| \frac{1}{4h_x h_y} \right|^2 dx dy = \frac{N}{4h_x h_y}$$

and  $\psi_j^h$  satisfies

$$\int_{\Omega} |\psi_1^h|^2 dx dy = \sum_{K \in T^h} \int_K \left( \frac{y_c + h_y - y}{4h_x h_y} \right)^2 dx dy = \sum_{K \in T^h} \frac{2h_x}{(4h_x h_y)^2} \cdot \frac{-1}{3} (y_c + h_y - y)^3 \Big|_{y=y_c-h_y}^{y_c+h_y} = \frac{Nh_y}{3h_x},$$

$$\int_{\Omega} |\psi_3^h|^2 dx dy = \frac{Nh_y}{3h_x}, \quad \int_{\Omega} |\psi_2^h|^2 dx dy = \int_{\Omega} |\psi_4^h|^2 dx dy = \frac{Nh_x}{3h_y},$$

from which we can see that

$$\frac{\|\nabla \times \psi_j^h\|_{0,\Omega}^2}{\|\psi_j^h\|_{0,\Omega}^2} = \frac{3}{4h_y^2}, \quad j = 1, 3.$$

Similarly, we have

$$\frac{\|\nabla \times \psi_j^h\|_{0,\Omega}^2}{\|\psi_j^h\|_{0,\Omega}^2} = \frac{3}{4h_x^2}, \quad j = 2, 4.$$

Denote  $h = \max\{h_x, h_y\}$ . Hence we have

$$c_{inv} \geq \sqrt{\frac{3}{4}} \frac{h}{h_x} \quad \text{or} \quad c_{inv} \geq \sqrt{\frac{3}{4}} \frac{h}{h_y}, \tag{32}$$

which means that  $c_{inv}$  can be very large for anisotropic meshes. But for the often used shape regular mesh,  $c_{inv}$  should not be that large. Of course, exact estimate of  $c_{inv}$  really depends on the mesh and the order of the basis functions. To our knowledge, there is no general formular for  $c_{inv}$ .

The rest of the section is devoted to the stability analysis on the cloak region  $\Omega_c = \Omega \setminus \Omega_r$ . For simplicity, in the rest of this section, we use  $\|\cdot\|_0$  to denote  $\|\cdot\|_{0,\Omega_c}$ .

**Lemma 4.1**

$$\begin{aligned} & \frac{\epsilon_0}{2} \left( \|\sqrt{\epsilon_\phi} \delta_\tau E_h^{n+\frac{1}{2}}\|_0^2 - \|\sqrt{\epsilon_\phi} \delta_\tau E_h^{n-\frac{1}{2}}\|_0^2 \right) + \frac{\epsilon_0 \omega_p^2}{2} \left( \|\sqrt{\epsilon_\phi} \widehat{E}_h^{n+\frac{1}{2}}\|_0^2 - \|\sqrt{\epsilon_\phi} \widehat{E}_h^{n-\frac{1}{2}}\|_0^2 \right) + \tau \gamma \epsilon_0 \|\sqrt{\epsilon_\phi} \delta_\tau \widehat{E}_h^{n+\frac{1}{2}}\|_0^2 \\ & \leq \tau \left( (M_A + \epsilon_\phi M_B) \delta_\tau^2 \widehat{D}_h^{n+\frac{1}{2}}, \delta_\tau \widehat{E}_h^{n+\frac{1}{2}} \right) + \tau \gamma \left( \delta_2 \left( (M_A + \epsilon_\phi M_B) \delta_\tau \widehat{D}_h^{n+\frac{1}{2}}, \delta_\tau \widehat{D}_h^{n+\frac{1}{2}} \right) + \frac{1}{4\delta_2} \left( (M_A + \epsilon_\phi M_B) \delta_\tau \widehat{E}_h^{n+\frac{1}{2}}, \delta_\tau \widehat{E}_h^{n+\frac{1}{2}} \right) \right) \\ & \quad + \frac{\tau \omega_p^2}{2} \left( \delta_3 \epsilon_0 \|\sqrt{\epsilon_\phi} \delta_\tau \widehat{E}_h^{n+\frac{1}{2}}\|_0^2 + \frac{1}{2\delta_3 \epsilon_0} \left( \|\widehat{D}_h^{n+\frac{1}{2}}\|_0^2 + \|\widehat{D}_h^{n-\frac{1}{2}}\|_0^2 \right) \right). \end{aligned} \tag{33}$$

**Proof.** Choosing  $\tilde{\phi}_h = \tau \delta_\tau \widehat{E}_h^{n+\frac{1}{2}}$  in (18), we obtain

$$\begin{aligned}
 (\epsilon_0 \epsilon_\phi \delta_\tau^2 \mathbf{E}_h^{n+\frac{1}{2}}, \tau \delta_\tau \widehat{\mathbf{E}}_h^{n+\frac{1}{2}}) &= \epsilon_0 (\epsilon_\phi (\delta_\tau \mathbf{E}_h^{n+\frac{1}{2}} - \delta_\tau \mathbf{E}_h^{n-\frac{1}{2}}), \delta_\tau \widehat{\mathbf{E}}_h^{n+\frac{1}{2}}) \\
 &= \frac{\epsilon_0}{2} \left( \|\sqrt{\epsilon_\phi} \delta_\tau \mathbf{E}_h^{n+\frac{1}{2}}\|_0^2 - \|\sqrt{\epsilon_\phi} \delta_\tau \mathbf{E}_h^{n-\frac{1}{2}}\|_0^2 \right), \\
 &\quad \left( \gamma \epsilon_0 \epsilon_\phi \frac{(\mathbf{E}_h^{n+\frac{1}{2}} - \mathbf{E}_h^{n-\frac{3}{2}})}{2\tau}, \tau \delta_\tau \widehat{\mathbf{E}}_h^{n+\frac{1}{2}} \right) \\
 &= \frac{\tau \gamma \epsilon_0}{2} (\epsilon_\phi (\delta_\tau \mathbf{E}_h^{n+\frac{1}{2}} + \delta_\tau \mathbf{E}_h^{n-\frac{1}{2}}), \delta_\tau \widehat{\mathbf{E}}_h^{n+\frac{1}{2}}) = \tau \gamma \epsilon_0 \|\sqrt{\epsilon_\phi} \delta_\tau \widehat{\mathbf{E}}_h^{n+\frac{1}{2}}\|_0^2, \\
 &\quad \left( \omega_p^2 \epsilon_0 \epsilon_\phi \frac{(\mathbf{E}_h^{n+\frac{1}{2}} + 2\mathbf{E}_h^{n-\frac{1}{2}} + \mathbf{E}_h^{n-\frac{3}{2}})}{4}, \widehat{\mathbf{E}}_h^{n+\frac{1}{2}} - \widehat{\mathbf{E}}_h^{n-\frac{1}{2}} \right) \\
 &= \frac{\epsilon_0 \omega_p^2}{2} \left( \|\sqrt{\epsilon_\phi} \widehat{\mathbf{E}}_h^{n+\frac{1}{2}}\|_0^2 - \|\sqrt{\epsilon_\phi} \widehat{\mathbf{E}}_h^{n-\frac{1}{2}}\|_0^2 \right).
 \end{aligned}$$

Using the facts that  $|M_A| \leq I, |M_B| \leq I$  and  $1 < \frac{R_2}{R_2 - R_1} \leq \epsilon_\phi$ , and the arithmetic–geometric mean inequality  $|ab| \leq \delta a^2 + \frac{1}{4\delta} b^2$ , we have

$$\begin{aligned}
 (\gamma(M_A + \epsilon_\phi M_B) \delta_{2\tau} \mathbf{D}_h^{n+\frac{1}{2}}, \tau \delta_\tau \widehat{\mathbf{E}}_h^{n+\frac{1}{2}}) &= \tau \gamma ((M_A + \epsilon_\phi M_B) \delta_\tau \widehat{\mathbf{D}}_h^{n+\frac{1}{2}}, \delta_\tau \widehat{\mathbf{E}}_h^{n+\frac{1}{2}}) \\
 &\leq \tau \gamma \left( \delta_2 ((M_A + \epsilon_\phi M_B) \delta_\tau \widehat{\mathbf{D}}_h^{n+\frac{1}{2}}, \delta_\tau \widehat{\mathbf{D}}_h^{n+\frac{1}{2}}) + \frac{1}{4\delta_2} ((M_A + \epsilon_\phi M_B) \delta_\tau \widehat{\mathbf{E}}_h^{n+\frac{1}{2}}, \delta_\tau \widehat{\mathbf{E}}_h^{n+\frac{1}{2}}) \right)
 \end{aligned}$$

and

$$\begin{aligned}
 \left( \omega_p^2 M_A \frac{\mathbf{D}_h^{n+\frac{1}{2}} + 2\mathbf{D}_h^{n-\frac{1}{2}} + \mathbf{D}_h^{n-\frac{3}{2}}}{4}, \tau \delta_\tau \widehat{\mathbf{E}}_h^{n+\frac{1}{2}} \right) &\leq \frac{\tau \omega_p^2}{2} \|\delta_\tau \widehat{\mathbf{E}}_h^{n+\frac{1}{2}}\|_0 \|\widehat{\mathbf{D}}_h^{n+\frac{1}{2}} + \widehat{\mathbf{D}}_h^{n-\frac{1}{2}}\|_0 \\
 &\leq \frac{\tau \omega_p^2}{2} \left( \delta_3 \epsilon_0 \|\sqrt{\epsilon_\phi} \delta_\tau \widehat{\mathbf{E}}_h^{n+\frac{1}{2}}\|_0^2 + \frac{1}{2\delta_3 \epsilon_0} \left( \|\widehat{\mathbf{D}}_h^{n+\frac{1}{2}}\|_0^2 + \|\widehat{\mathbf{D}}_h^{n-\frac{1}{2}}\|_0^2 \right) \right),
 \end{aligned}$$

where in the last step, we used the fact that  $\|\delta_\tau \widehat{\mathbf{E}}_h^{n+\frac{1}{2}}\| \leq \|\sqrt{\epsilon_\phi} \delta_\tau \widehat{\mathbf{E}}_h^{n+\frac{1}{2}}\|_0$ .

The proof completes by adding the above inequalities together.  $\square$

**Lemma 4.2**

$$\begin{aligned}
 &\frac{1}{2} \mu_0 A \left[ ((M_A + \epsilon_\phi M_B) \delta_\tau H_h^{n+1}, \delta_\tau H_h^{n+1}) - ((M_A + \epsilon_\phi M_B) \delta_\tau H_h^n, \delta_\tau H_h^n) \right] + \tau \mu_0 A \gamma_m ((M_A + \epsilon_\phi M_B) \delta_\tau \widehat{H}_h^{n+1}, \delta_\tau \widehat{H}_h^{n+1}) \\
 &\quad + \frac{\mu_0 A \omega_{pm}^2}{2} \left[ ((M_A + \epsilon_\phi M_B) \widehat{H}_h^{n+1}, \widehat{H}_h^{n+1}) - ((M_A + \epsilon_\phi M_B) \widehat{H}_h^n, \widehat{H}_h^n) \right] \\
 &\leq \tau \gamma_m \left[ \delta_8 ((M_A + \epsilon_\phi M_B) \delta_\tau \widehat{B}_h^{n+1}, \delta_\tau \widehat{B}_h^{n+1}) + \frac{1}{4\delta_8} ((M_A + \epsilon_\phi M_B) \delta_\tau \widehat{H}_h^{n+1}, \delta_\tau \widehat{H}_h^{n+1}) \right] + \tau ((M_A + \epsilon_\phi M_B) \delta_\tau^2 B_h^{n+1}, \delta_\tau \widehat{H}_h^{n+1}).
 \end{aligned} \tag{34}$$

**Proof.** An equivalent variable coefficient form of (20) can be written as

$$\begin{aligned}
 &((M_A + \epsilon_\phi M_B) (\mu_0 A \delta_\tau^2 H_h^{n+1} + \mu_0 A \gamma_m \delta_{2\tau} H_h^{n+1} + \mu_0 A \omega_{pm}^2 \widehat{H}_h^n), \tilde{\psi}_h) \\
 &= \left[ (M_A + \epsilon_\phi M_B) \delta_\tau^2 B_h^{n+1}, \tilde{\psi}_h \right] + \left[ (M_A + \epsilon_\phi M_B) \gamma_m \delta_{2\tau} B_h^{n+1}, \tilde{\psi}_h \right].
 \end{aligned} \tag{35}$$

Choosing  $\tilde{\psi}_h = \tau \delta_\tau \widehat{H}_h^{n+1}$  in (35), we obtain

$$\begin{aligned}
 \mu_0 A ((M_A + \epsilon_\phi M_B) (\delta_\tau H_h^{n+1} - \delta_\tau H_h^n), \delta_\tau \widehat{H}_h^{n+1}) &= \frac{1}{2} \mu_0 A \left( ((M_A + \epsilon_\phi M_B) \delta_\tau H_h^{n+1}, \delta_\tau H_h^{n+1}) - ((M_A + \epsilon_\phi M_B) \delta_\tau H_h^n, \delta_\tau H_h^n) \right), \\
 \mu_0 A \gamma_m ((M_A + \epsilon_\phi M_B) \delta_{2\tau} H_h^{n+1}, \tau \delta_\tau \widehat{H}_h^{n+1}) &= \tau \mu_0 A \gamma_m ((M_A + \epsilon_\phi M_B) \delta_\tau \widehat{H}_h^{n+1}, \delta_\tau \widehat{H}_h^{n+1}), \\
 \frac{\mu_0 A \omega_{pm}^2}{4} ((M_A + \epsilon_\phi M_B) (H_h^{n+1} + H_h^n + H_h^{n-1}), \widehat{H}_h^{n+1} - \widehat{H}_h^n) &= \frac{\mu_0 A \omega_{pm}^2}{2} \left[ ((M_A + \epsilon_\phi M_B) \widehat{H}_h^{n+1}, \widehat{H}_h^{n+1}) - ((M_A + \epsilon_\phi M_B) \widehat{H}_h^n, \widehat{H}_h^n) \right], \\
 \gamma_m ((M_A + \epsilon_\phi M_B) \delta_{2\tau} B_h^{n+1}, \tau \delta_\tau \widehat{H}_h^{n+1}) &= \tau \gamma_m ((M_A + \epsilon_\phi M_B) \delta_\tau \widehat{B}_h^{n+1}, \delta_\tau \widehat{H}_h^{n+1}) \\
 &\leq \tau \gamma_m \left[ \delta_8 ((M_A + \epsilon_\phi M_B) \delta_\tau \widehat{B}_h^{n+1}, \delta_\tau \widehat{B}_h^{n+1}) + \frac{1}{4\delta_8} ((M_A + \epsilon_\phi M_B) \delta_\tau \widehat{H}_h^{n+1}, \delta_\tau \widehat{H}_h^{n+1}) \right].
 \end{aligned}$$

Summing up the above estimates concludes the proof.  $\square$

**Lemma 4.3**

$$\begin{aligned} & \tau \left( (M_A + \epsilon_\phi M_B) \delta_\tau^2 \mathbf{D}_h^{n+\frac{1}{2}}, \delta_\tau \widehat{\mathbf{E}}_h^{n+\frac{1}{2}} \right) + \tau \left( (M_A + \epsilon_\phi M_B) \delta_\tau^2 \mathbf{B}_h^{n+1}, \delta_\tau \widehat{H}_h^{n+1} \right) \\ &= \frac{\tau}{2} \left[ \left( (M_A + \epsilon_\phi M_B) \delta_\tau H_h^n, \nabla \times \delta_\tau \mathbf{E}_h^{n-\frac{1}{2}} \right) - \left( (M_A + \epsilon_\phi M_B) \delta_\tau H_h^{n+1}, \nabla \times \delta_\tau \mathbf{E}_h^{n+\frac{1}{2}} \right) \right] \\ & \quad + \tau \left( \delta_\tau H_h^n, \nabla (M_A + \epsilon_\phi M_B) \times \delta_\tau \widehat{\mathbf{E}}_h^{n+\frac{1}{2}} \right). \end{aligned} \tag{36}$$

**Proof.** For an arbitrary function  $f(x)$ , multiplying (2) by  $f(x)\phi$  and integrating over  $\Omega$ , we can obtain

$$\left( f(\mathbf{x}) \frac{\partial \mathbf{D}}{\partial t}, \phi \right) = (\nabla \times H, f(\mathbf{x})\phi) = (H, \nabla \times (f(\mathbf{x})\phi)), \quad \forall \phi \in H_0(\text{curl}; \Omega), \tag{37}$$

from which we can obtain an equivalent form of (17):

$$\left( f(\mathbf{x}) \delta_\tau \mathbf{D}_h^{n+\frac{1}{2}}, \phi_h \right) - (H_h^n, \nabla \times (f(\mathbf{x})\phi_h)) = 0, \quad \forall \phi_h \in \mathbf{V}_h^0. \tag{38}$$

Subtracting (38) from itself with  $n$  reduced by 1, then dividing by  $\tau$ , we obtain

$$\left( f(\mathbf{x}) \delta_\tau^2 \mathbf{D}_h^{n+\frac{1}{2}}, \phi_h \right) - (\delta_\tau H_h^n, \nabla \times (f(\mathbf{x})\phi_h)) = 0, \quad \forall \phi_h \in \mathbf{V}_h^0. \tag{39}$$

On the other hand, it is easy to see that an equivalent form of (19) is:

$$\left( f(\mathbf{x}) \delta_\tau \mathbf{B}_h^{n+1}, \psi_h \right) + \left( f(\mathbf{x}) \nabla \times \mathbf{E}_h^{n+\frac{1}{2}}, \psi_h \right) = 0, \quad \forall \psi_h \in \mathbf{U}_h, \tag{40}$$

from which we obtain

$$\left( f(\mathbf{x}) \delta_\tau^2 \mathbf{B}_h^{n+1}, \psi_h \right) + \left( f(\mathbf{x}) \nabla \times \delta_\tau \mathbf{E}_h^{n+\frac{1}{2}}, \psi_h \right) = 0, \quad \forall \psi_h \in \mathbf{U}_h. \tag{41}$$

Choosing  $\phi_h = \tau \delta_\tau \widehat{\mathbf{E}}_h^{n+\frac{1}{2}}$ ,  $\psi_h = \tau \delta_\tau \widehat{H}_h^{n+1}$  in (39) and (41), respectively, we have

$$\tau \left( f(\mathbf{x}) \delta_\tau^2 \mathbf{D}_h^{n+\frac{1}{2}}, \delta_\tau \widehat{\mathbf{E}}_h^{n+\frac{1}{2}} \right) + \tau \left( f(\mathbf{x}) \delta_\tau^2 \mathbf{B}_h^{n+1}, \delta_\tau \widehat{H}_h^{n+1} \right) = \tau \left[ (\delta_\tau H_h^n, \nabla \times (f(\mathbf{x}) \delta_\tau \mathbf{E}_h^{n+\frac{1}{2}})) - (f(\mathbf{x}) \nabla \times \delta_\tau \widehat{\mathbf{E}}_h^{n+\frac{1}{2}}, \delta_\tau \widehat{H}_h^{n+1}) \right]. \tag{42}$$

Using the identity

$$\left( \delta_\tau H_h^n, f(\mathbf{x}) \nabla \times \delta_\tau \widehat{\mathbf{E}}_h^{n+\frac{1}{2}} \right) - \left( f(\mathbf{x}) \nabla \times \delta_\tau \mathbf{E}_h^{n+\frac{1}{2}}, \delta_\tau \widehat{H}_h^{n+1} \right) = \frac{1}{2} \left[ (\delta_\tau H_h^n, f(\mathbf{x}) \nabla \times \delta_\tau \mathbf{E}_h^{n-\frac{1}{2}}) - (\delta_\tau H_h^{n+1}, f(\mathbf{x}) \nabla \times \delta_\tau \mathbf{E}_h^{n+\frac{1}{2}}) \right], \tag{43}$$

the formula

$$\nabla \times (f(\mathbf{x})\mathbf{u}) = f(\mathbf{x})\nabla \times \mathbf{u} + \nabla f(\mathbf{x}) \times \mathbf{u}$$

and choosing  $f(x) = M_A + \epsilon_\phi M_B$  in (42), we conclude the proof.  $\square$

**Lemma 4.4.** For any vector  $(u, v)$ , we have

$$(u, v)(M_A + \epsilon_\phi M_B) \begin{pmatrix} u \\ v \end{pmatrix} > u^2 + v^2.$$

**Proof.** Using the definitions of  $M_A$  and  $M_B$ , and the fact that  $\epsilon_\phi > 1$ , we have

$$\begin{aligned} (u, v)(M_A + \epsilon_\phi M_B) \begin{pmatrix} u \\ v \end{pmatrix} &= (u^2 \sin^2 \phi - 2uv \sin \phi \cos \phi + v^2 \cos^2 \phi) + \epsilon_\phi (u^2 \cos^2 \phi + 2uv \sin \phi \cos \phi + v^2 \sin^2 \phi) \\ &= (u \sin \phi - v \cos \phi)^2 + \epsilon_\phi (u \cos \phi + v \sin \phi)^2 > (u \sin \phi - v \cos \phi)^2 + (u \cos \phi + v \sin \phi)^2 \\ &= u^2 + v^2. \quad \square \end{aligned}$$

Combining the above estimates, we finally have the following stability result on the cloaking region:

**Theorem 4.2.** Under the time step constraint (27), for any  $N \geq 1$ , we have

$$\begin{aligned} & \epsilon_0 \left( \left\| \sqrt{\epsilon_\phi} \delta_\tau \mathbf{E}_h^{N+\frac{1}{2}} \right\|_0^2 + \omega_p^2 \left\| \sqrt{\epsilon_\phi} \widehat{\mathbf{E}}_h^{N+\frac{1}{2}} \right\|_0^2 \right) + \mu_0 A \left( \left\| \delta_\tau H_h^{N+1} \right\|_0^2 + \omega_{pm}^2 \left\| \widehat{H}_h^{N+1} \right\|_0^2 \right) \\ & \leq C \left[ \epsilon_0 \left\| \sqrt{\epsilon_\phi} \delta_\tau \mathbf{E}_h^{\frac{1}{2}} \right\|_0^2 + \epsilon_0 \omega_p^2 \left\| \sqrt{\epsilon_\phi} \widehat{\mathbf{E}}_h^{\frac{1}{2}} \right\|_0^2 + \mu_0 A \left\| \sqrt{\epsilon_\phi} \delta_\tau H_h^1 \right\|_0^2 + \mu_0 A \omega_{pm}^2 \left\| \sqrt{\epsilon_\phi} \widehat{H}_h^1 \right\|_0^2 \right]. \end{aligned}$$

**Proof.** Summing up (33) and (34) from  $n = 1$  to  $N \geq 1$  and using (36), we obtain

$$\begin{aligned}
 & \frac{\epsilon_0}{2} \left( \left\| \sqrt{\epsilon_\phi} \delta_\tau \mathbf{E}_h^{N+\frac{1}{2}} \right\|_0^2 - \left\| \sqrt{\epsilon_\phi} \delta_\tau \mathbf{E}_h^1 \right\|_0^2 \right) + \frac{\epsilon_0 \omega_p^2}{2} \left( \left\| \sqrt{\epsilon_\phi} \widehat{\mathbf{E}}_h^{N+\frac{1}{2}} \right\|_0^2 - \left\| \sqrt{\epsilon_\phi} \widehat{\mathbf{E}}_h^1 \right\|_0^2 \right) + \tau \gamma \epsilon_0 \sum_{n=1}^N \left\| \sqrt{\epsilon_\phi} \delta_\tau \widehat{\mathbf{E}}_h^{n+\frac{1}{2}} \right\|_0^2 \\
 & + \frac{1}{2} \mu_0 A \left[ \left( (M_A + \epsilon_\phi M_B) \delta_\tau H_h^{N+1}, \delta_\tau H_h^{N+1} \right) - \left( (M_A + \epsilon_\phi M_B) \delta_\tau H_h^1, \delta_\tau H_h^1 \right) \right] + \tau \mu_0 A \gamma_m \sum_{n=1}^N \left( (M_A + \epsilon_\phi M_B) \delta_\tau \widehat{H}_h^{n+1}, \delta_\tau \widehat{H}_h^{n+1} \right) \\
 & + \frac{\mu_0 A \omega_{pm}^2}{2} \left[ \left( (M_A + \epsilon_\phi M_B) \widehat{H}_h^{N+1}, \widehat{H}_h^{N+1} \right) - \left( (M_A + \epsilon_\phi M_B) \widehat{H}_h^1, \widehat{H}_h^1 \right) \right] \\
 & \leq \frac{\tau}{2} \left[ \left( (M_A + \epsilon_\phi M_B) \delta_\tau H_h^1, \nabla \times \delta_\tau \mathbf{E}_h^1 \right) - \left( (M_A + \epsilon_\phi M_B) \delta_\tau H_h^{N+1}, \nabla \times \delta_\tau \mathbf{E}_h^{N+\frac{1}{2}} \right) \right] + \tau \sum_{n=1}^N \left( \delta_\tau H_h^n, \nabla (M_A + \epsilon_\phi M_B) \times \delta_\tau \widehat{\mathbf{E}}_h^{n+\frac{1}{2}} \right) \\
 & + \tau \gamma \sum_{n=1}^N \left( \delta_2 \left( (M_A + \epsilon_\phi M_B) \delta_\tau \widehat{\mathbf{D}}_h^{n+\frac{1}{2}}, \delta_\tau \widehat{\mathbf{D}}_h^{n+\frac{1}{2}} \right) + \frac{1}{4\delta_2} \left( (M_A + \epsilon_\phi M_B) \delta_\tau \widehat{\mathbf{E}}_h^{n+\frac{1}{2}}, \delta_\tau \widehat{\mathbf{E}}_h^{n+\frac{1}{2}} \right) \right) \\
 & + \tau \gamma_m \sum_{n=1}^N \left[ \delta_8 \left( (M_A + \epsilon_\phi M_B) \delta_\tau \widehat{B}_h^{n+1}, \delta_\tau \widehat{B}_h^{n+1} \right) + \frac{1}{4\delta_8} \left( (M_A + \epsilon_\phi M_B) \delta_\tau \widehat{H}_h^{n+1}, \delta_\tau \widehat{H}_h^{n+1} \right) \right] \\
 & + \frac{\tau \omega_p^2}{2} \sum_{n=1}^N \left( \delta_3 \epsilon_0 \left\| \sqrt{\epsilon_\phi} \delta_\tau \widehat{\mathbf{E}}_h^{n+\frac{1}{2}} \right\|_0^2 + \frac{1}{2\delta_3 \epsilon_0} \left( \left\| \widehat{\mathbf{D}}_h^{n+\frac{1}{2}} \right\|_0^2 + \left\| \widehat{\mathbf{D}}_h^{n-\frac{1}{2}} \right\|_0^2 \right) \right). \tag{44}
 \end{aligned}$$

Adding (17) to itself by reducing  $n$  by one, we have

$$\left( \delta_\tau \widehat{\mathbf{D}}_h^{n+\frac{1}{2}}, \phi_h \right) - \left( \widehat{H}_h^n, \nabla \times \phi_h \right) = 0. \tag{45}$$

Then choosing  $\phi_h = \delta_\tau \widehat{\mathbf{D}}_h^{n+\frac{1}{2}}$  in (45) and using the inverse estimate (26), we have

$$\left\| \delta_\tau \widehat{\mathbf{D}}_h^{n+\frac{1}{2}} \right\|_0 \leq c_{inv} h^{-1} \left\| \widehat{H}_h^n \right\|_0. \tag{46}$$

By the same technique, from (19), we can obtain

$$\left\| \delta_\tau \widehat{B}_h^{n+1} \right\|_0 \leq c_{inv} h^{-1} \left\| \widehat{\mathbf{E}}_h^{n+\frac{1}{2}} \right\|_0. \tag{47}$$

Similarly, choosing  $\phi_h = \frac{\tau}{\epsilon_0} \widehat{\mathbf{D}}_h^{n+\frac{1}{2}}$  in (45) and using the inequality  $(a - b)a \geq \frac{1}{2}(a^2 - b^2)$ , we have

$$\begin{aligned}
 \frac{1}{2\epsilon_0} \left( \left\| \widehat{\mathbf{D}}_h^{n+\frac{1}{2}} \right\|_0^2 - \left\| \widehat{\mathbf{D}}_h^{n-\frac{1}{2}} \right\|_0^2 \right) & \leq \frac{\tau}{\epsilon_0} \left( \widehat{H}_h^n, \nabla \times \widehat{\mathbf{D}}_h^{n+\frac{1}{2}} \right) \leq \frac{\tau c_{inv}}{h \epsilon_0} \left\| \widehat{H}_h^n \right\|_0 \left\| \widehat{\mathbf{D}}_h^{n+\frac{1}{2}} \right\|_0 = \frac{\tau c_{inv} c_v}{h} \sqrt{\mu_0} \left\| \widehat{H}_h^n \right\|_0 \cdot \frac{1}{\sqrt{\epsilon_0}} \left\| \widehat{\mathbf{D}}_h^{n+\frac{1}{2}} \right\|_0 \\
 & \leq \frac{\tau c_{inv} \tau c_v}{h} \left( \delta_9 \mu_0 \left\| \widehat{H}_h^n \right\|_0^2 + \frac{1}{4\delta_9 \epsilon_0} \left\| \widehat{\mathbf{D}}_h^{n+\frac{1}{2}} \right\|_0^2 \right). \tag{48}
 \end{aligned}$$

Furthermore, by Lemma 4.4, we know that

$$\left( (M_A + \epsilon_\phi M_B) \delta_\tau \widehat{H}_h^{N+1}, \delta_\tau \widehat{H}_h^{N+1} \right) > \left\| \delta_\tau \widehat{H}_h^{N+1} \right\|_0^2.$$

Similar estimates hold true for other terms.

The proof is completed by substituting the above estimates to (44), then choosing  $\tau$  satisfying the constraint (27),  $\delta_i$  properly so that all terms can be controlled by the left hand side terms, and using the discrete Gronwall inequality.  $\square$

### 5. Numerical tests

In this section, we present a numerical simulation of a cylindrical cloak obtained by our FETD algorithm. The cloak simulation setup is shown in Fig. 1(a), where the cloaked object is hidden inside a perfectly electrically conducting (PEC) cylinder with radius  $R_1$  meter (m), the object is wrapped by a cylindrical cloak with thickness  $R_2 - R_1$ .

In our cloak simulation, we use  $R_1 = 0.1$  m,  $R_2 = 0.2$  m, and consider the ideal lossless case, i.e.  $\gamma = \gamma_m = 0$  in our Drude model. A plane wave source is specified by the function  $H_z = 0.1 \sin(\omega t)$ , where  $\omega = 2\pi f$  with operating frequency  $f = 2.0$  GHz. The parameters  $\omega_p = \omega_{pm}$  is calculated by the Drude model  $\omega_p = \omega \sqrt{1 - \epsilon_r}$ .

To accommodate the PML easily, we used a mixed mesh shown in Fig. 1(b). Our tests showed that in order to see the cloaking phenomenon, the mesh has to be fine enough. In our results presented below, the mesh is obtained by uniformly refining the one given in Fig. 1(b) four times, in which case the total number of edges used are 623,808, the DOFs for  $\mathbf{E}$  is 621,376, the total numbers of triangular elements and rectangular elements are 262,144 and 114,688, respectively. Hence the DOFs for  $H$  is 376,832. The time step is chosen as  $\tau = 0.1$  ps, and the total number of time steps is 50,000, i.e.

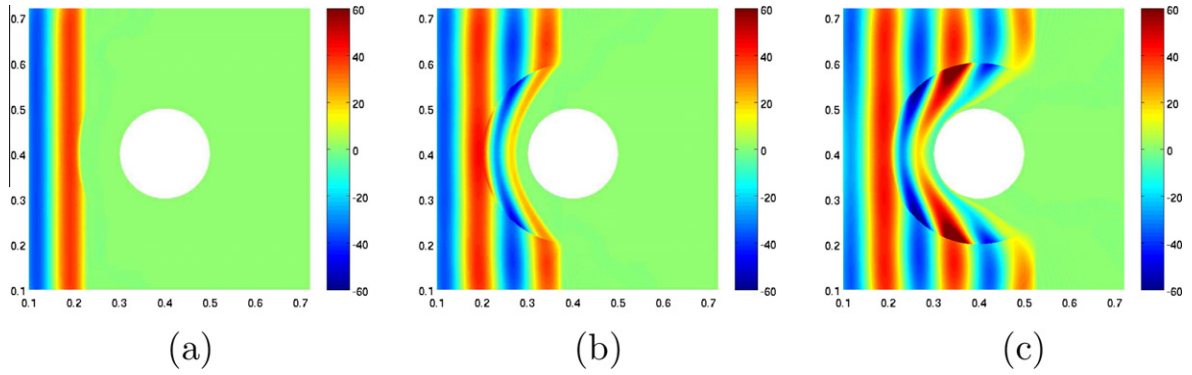


Fig. 2.  $E_y$  at (a)  $t = 0.5$  ns; (b)  $t = 1.0$  ns; and (c)  $t = 1.5$  ns.

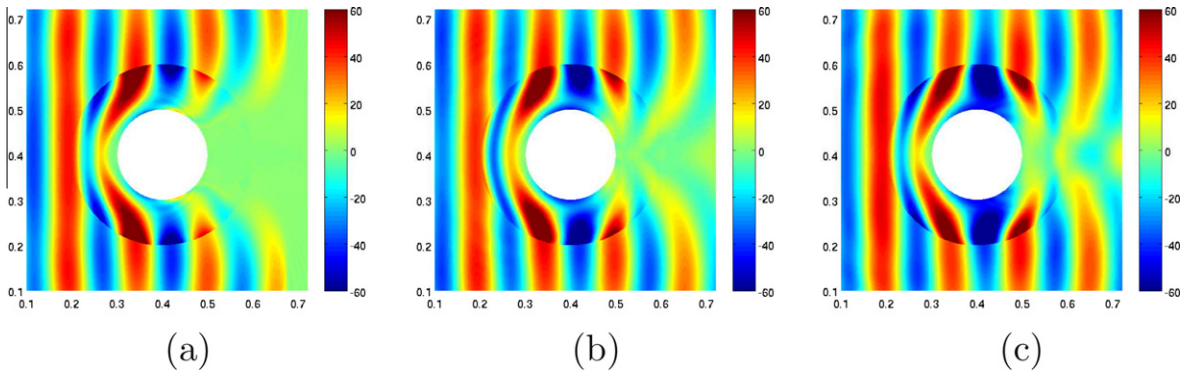


Fig. 3.  $E_y$  at (a)  $t = 2.0$  ns; (b)  $t = 2.5$  ns; and (c)  $t = 3.0$  ns.

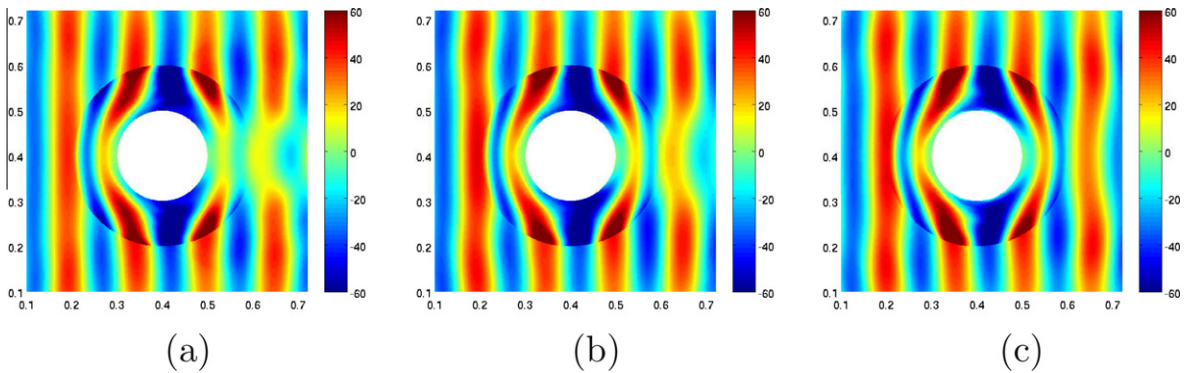


Fig. 4.  $E_y$  at (a)  $t = 3.5$  ns; (b)  $t = 4.0$  ns; and (c)  $t = 4.5$  ns.

$T = 5.0$  ns. Our algorithm is implemented under MATLAB 7.0 running on a Dell desktop with 2 GB memory and 2.93 GHz CPU. The average CPU time for each time step is about 16 s.

To see how wave propagated in the cloak structure, we plotted the  $E_y$  fields at every 5000 time steps in Figs. 2–4, which show clearly how wave gets distorted in the cloak region. After about 40,000 time steps, the plane-wave shape gets restored, which renders the object placed inside the cloak invisible to external electromagnetic fields. We plotted all fields obtained at the final simulation time  $T = 5$  ns in Fig. 5. Note that our results are similar to that obtained by the FDTD method [31] and by the frequency domain methods [6,17].

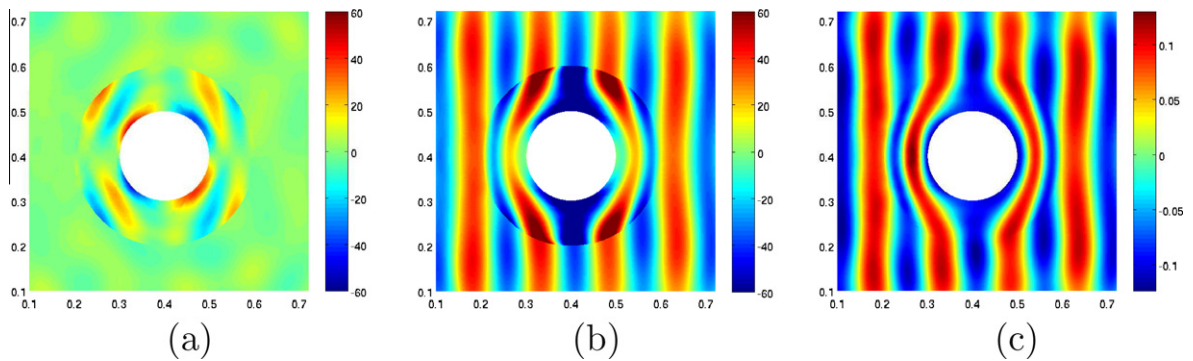


Fig. 5. All fields obtained at  $T = 5.0$  ns: (a)  $E_x$ ; (b)  $E_y$ ; and (c)  $H_z$ .

## 6. Conclusions

In conclusion, we have proposed a time-domain finite element method for modeling of 2-D cylindrical cloaks. The stability of the proposed method is investigated, and the algorithm is implemented for an ideal lossless cloak model. The simulation results from our algorithm match well with those obtained by the FDTD method [31]. This paper has demonstrated the effectiveness of FETD method for modeling of electromagnetic cloaks. More efficient algorithms such as multiscale technique [29], discontinuous Galerkin methods [11,12,15,16] and hp adaptive finite element methods [7] will be investigated in the future. Applications of FETD methods to other cloaking models [4,27] will be explored also.

## Acknowledgments

We like to thank anonymous referees for their insightful comments that improved the paper.

## References

- [1] A. Alú, N. Engheta, Achieving transparency with plasmonic and metamaterial coatings, *Phys. Rev. E* 72 (2005) 016623.
- [2] J.P. Berenger, A perfectly matched layer for the absorption of electromagnetic waves, *J. Comput. Phys.* 114 (1994) 185–200.
- [3] W. Cai, V. Shalaev, *Optical Metamaterials: Fundamentals and Applications*, Springer, 2009.
- [4] H. Chen, C.T. Chan, P. Sheng, Transformation optics and metamaterials, *Nature Materials* 9 (2010) 387–396.
- [5] P. Collins, J. McGuirk, A novel methodology for deriving improved material parameter sets for simplified cylindrical cloaks, *J. Opt. A Pure Appl. Opt.* 11 (2009) 015104.
- [6] S.A. Cummer, B.-I. Popa, D. Schurig, D.R. Smith, J. Pendry, Full-wave simulations of electromagnetic cloaking structures, *Phys. Rev. E* 74 (2006) 036621.
- [7] L. Demkowicz, J. Kurtz, D. Pardo, M. Paszynski, W. Rachowicz, A. Zdunek, Computing with hp Finite Elements. II. *Frontiers: Three-Dimensional Elliptic and Maxwell Problems with Applications*, Chapman & Hall, CRC, 2007.
- [8] N. Engheta, R.W. Ziolkowski (Eds.), *Electromagnetic Metamaterials: Physics and Engineering Explorations*, Wiley IEEE Press, Hoboken, NJ, 2006.
- [9] A. Greenleaf, Y. Kurylev, M. Lassas, G. Uhlmann, Cloaking devices, electromagnetics wormholes and transformation optics, *SIAM Rev.* 51 (2009) 3–33.
- [10] Y. Hao, R. Mittra, *FDTD Modeling of Metamaterials: Theory and Applications*, Artech House Publishers, 2008.
- [11] J.S. Hesthaven, T. Warburton, High-order nodal methods on unstructured grids. I. Time-domain solution of Maxwell's equations, *J. Comput. Phys.* 181 (2002) 186–221.
- [12] Y. Huang, J. Li, W. Yang, Interior penalty DG methods for Maxwell's equations in dispersive media, *J. Comput. Phys.* 230 (2011) 4559–4570.
- [13] R.V. Kohn, D. Onofrei, M.S. Vogelius, M.I. Weinstein, Cloaking via change of variables for the Helmholtz equation, *Commun. Pure Appl. Math.* 63 (2010) 0973–1016.
- [14] U. Leonhardt, Optical conformal mapping, *Science* 312 (2006) 1777–1780.
- [15] J. Li, Optimal L2 error estimates for the interior penalty DG method for Maxwell's equations in cold plasma, *Commun. Comput. Phys.* 11 (2012) 319–334.
- [16] J. Li, Posteriori error estimation for an interior penalty discontinuous Galerkin method for Maxwell's equations in cold plasma, *Adv. Appl. Math. Mech.* 1 (2009) 107–124.
- [17] J. Li, Y. Huang, Mathematical Simulation of cloaking metamaterial structures, *Adv. Appl. Math. Mech.* 4 (2012) 93–101.
- [18] J. Li, A. Wood, Finite element analysis for wave propagation in double negative metamaterials, *J. Sci. Comput.* 32 (2007) 263–286.
- [19] H. Liu, T. Zhou, On approximate electromagnetic cloaking by transformation media, *SIAM J. Appl. Math.* 71 (2011) 218–241.
- [20] R. Liu, C. Ji, J.J. Mock, J.Y. Chin, T.J. Cui, D.R. Smith, Broadband ground-plane cloak, *Science* 323 (2009) 366–369.
- [21] J. McGuirk, P. Collins, M. Havrilla, A. Wood, A Green's function approach to calculate scattering width for cylindrical cloaks, *Appl. Comput. Electromagn. Soc. J.* 25 (2010) 108–116.
- [22] G.W. Milton, M. Briane, J.R. Willis, On cloaking for elasticity and physical equations with a transformation invariant form, *New J. Phys.* 8 (2006) 248.
- [23] P. Monk, *Finite Element Methods for Maxwell's Equations*, Oxford University Press, 2003.
- [24] J.C. Nédélec, Mixed finite elements in  $R^3$ , *Numer. Math.* 35 (1998) 315–341.
- [25] J.B. Pendry, D. Schurig, D.R. Smith, Controlling electromagnetic fields, *Science* 312 (2006) 1780–1782.
- [26] D. Schurig, J.J. Mock, B.J. Justice, S.A. Cummer, J.B. Pendry, A.F. Starr, D.R. Smith, Metamaterial electromagnetic cloak at microwave frequencies, *Science* 314 (2006) 977–980.
- [27] Y.B. Zhai, X.W. Ping, W.X. Jiang, T.J. Cui, Finite-element analysis of three-dimensional axisymmetrical invisibility cloaks and other metamaterial devices, *Commun. Comput. Phys.* 8 (2010) 823–834.
- [28] J. Zhang, J. Huangfu, Y. Luo, H. Chen, J.A. Kong, B.-I. Wu, Cloak for multilayered and gradually changing media, *Phys. Rev. B* 77 (2008) 035116.
- [29] Y. Zhang, L. Cao, W. Allegretto, Y. Lin, Multiscale numerical algorithm for 3D Maxwell's equations with memory effects in composite materials, *Int. J. Numer. Anal. Model. Ser. B* 1 (2011) 41–57.

- [30] S. Zhao, G.W. Wei, High-order FDTD methods via derivative matching for Maxwell's equations with material interface, *J. Comput. Phys.* 200 (2004) 60–103.
- [31] Y. Zhao, C. Argyropoulos, Y. Hao, Full-wave finite-difference time-domain simulation of electromagnetic cloaking structures, *Optics Expr.* 16 (2008) 6717–6730.
- [32] Y. Zhao, Y. Hao, Full-wave parallel dispersive finite-difference time-domain modeling of three-dimensional electromagnetic cloaking structures, *J. Comput. Phys.* 228 (2009) 7300–7312.